

# **Study of wrinkles in film/substrate systems using Finite Element Method**

**P. Ventura<sup>1</sup>, M. Potier-Ferry<sup>1</sup>, H. Rezgui Chaabouni<sup>2</sup>, F. Xu<sup>3</sup>, A. Lejeune<sup>4</sup>**

<sup>1</sup>Laboratoire LEM3, Université de Lorraine, Metz, France

<sup>2</sup>GEMH, Université de Limoges, Egletons, France

<sup>3</sup>Institute of Mechanics and Computational Engineering, Dept. of Aeronautics  
and Astronautics, Fudan University, Shanghai, P. R. China

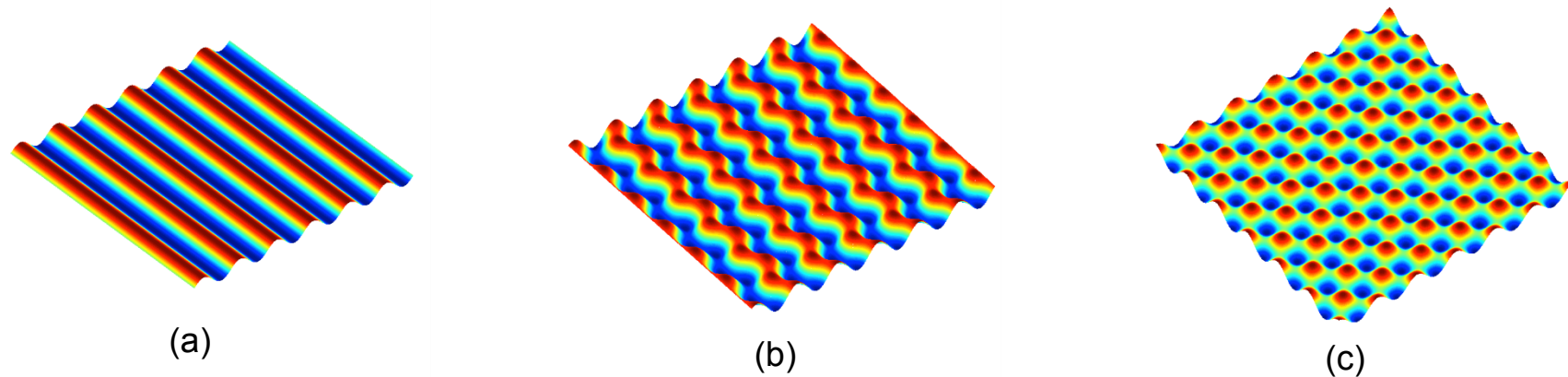
<sup>4</sup>Dept of Applied Mechanics / FEMTO-ST institute, UMR CNRS 6174,  
Besançon, France

# Outlines

- Introduction
- Geometry and 2D mechanical model
- Solution using Asymptotic Numerical Method (ANM)
- Implementation of the 2D FEM using FreeFem++
- Numerical results - 2D model
- Generalization to 3D
- Conclusions

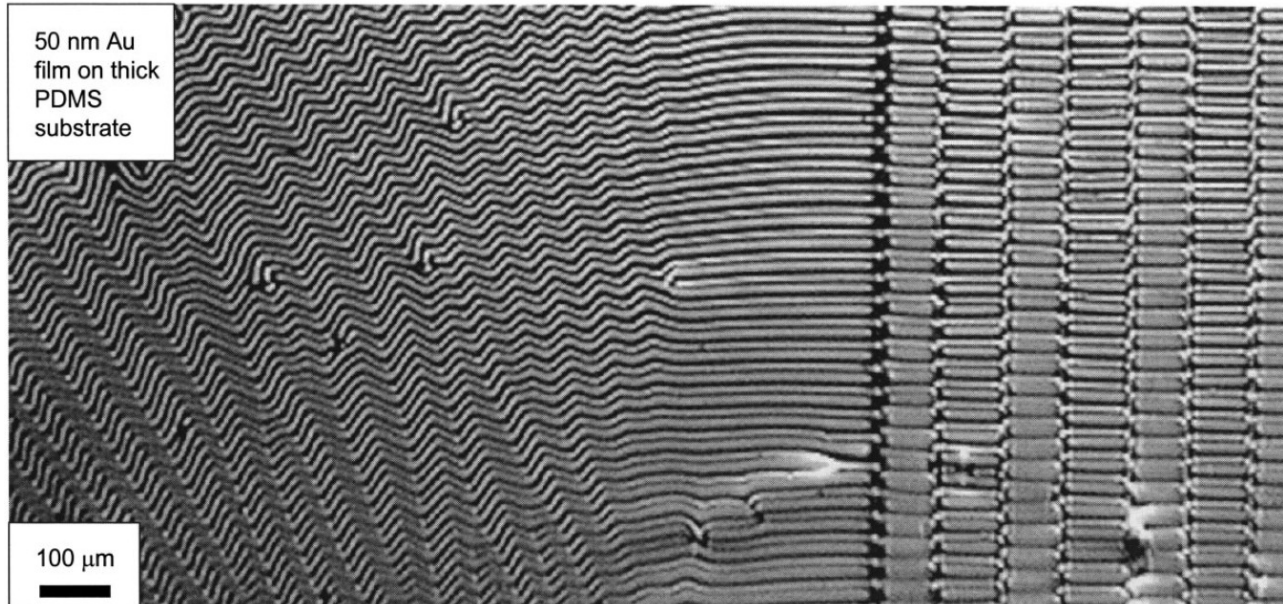
# Introduction

- Stiff thin film deposited on a polymer soft substrate:
  - Large difference of thermal dilatation between the film and substrate during the decrease of the temperature
  - resulting in compressive residual stresses which relax in creating surface wrinkles (Bowden, 1998, 1999)
- Depending on the mechanical and thermal stresses and on the boundary conditions, the film buckling may create sinusoidal (a), checkerboard (b) or herringbone modes (c)



# Introduction

- Surface wrinkles may be used in the industry for :
  - micro/nano fabrication of flexible electronic devices with morphological shapes (Bowden, 1999, et Wang, 2008)



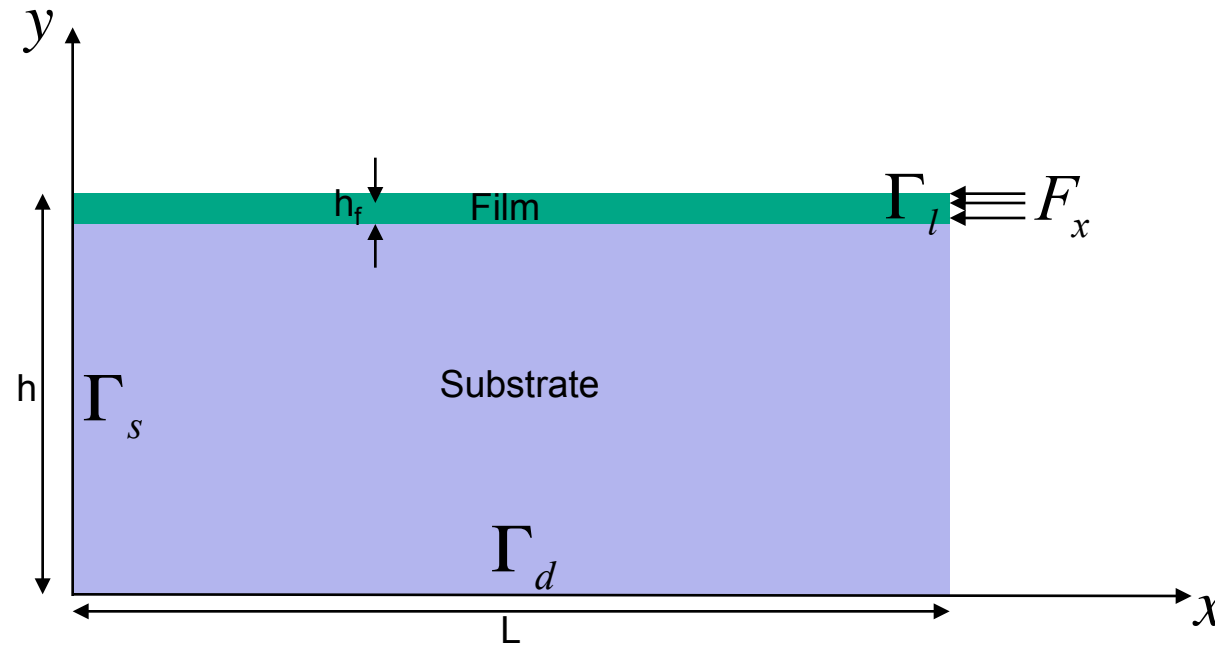
Buckling of 50 nm gold film deposited on a PDMS thick substrate which requires HPC (Bowden, 1998)

- Measurement of mechanical properties of materials (Howarter, 2010)

# Introduction

- **spectral methods**, using FFT, allows to obtain very good CPU times but need periodic boundary conditions (Z. Y. Huang, 2004)
- **Finite element method**, allows to take into account complex geometries and every kind of boundary conditions and also competitive CPU time using parallel code.
- Study of the loading behavior using **Asymptotic Numerical Method (ANM)** :
  - Taylor series expansion of displacement and loading parameter with respect to a path parameter.
- B. Cochelin, N. Damil, M. Potier-Ferry, Méthode Asymptotique Numérique, Hermès Lavoisier, 2007.
- Efficient 2D parallel (mpi) code implemented en **FreeFem++** wih the help of Frederic Hecht

# Geometry and 2D numerical model



- 2D plain strain assumption
- $y$  axis is a symmetrical axis of the problem
- Vertical displacement is assumed zero on  $\Gamma_d$  and  $\Gamma_l$
- $L = 1.5 \text{ mm}$ ,  $h = 0.1 \text{ mm}$ , et  $h_f = 0.001 \text{ mm}$
- Young modulus and Poisson coefficient :
  - Substrate :  $E_s = 1.8 \text{ Mpa}$ ,  $\nu_s = 0.48$
  - Film :  $E_f = 1.3 \cdot 10^5 \text{ Mpa}$ ,  $\nu_f = 0.3$

# Geometry and 2D numerical model

● Assumptions of the mechanical model :  $E_f$  ?  $E_s$

- Geometrical non linearity in the film
- Linear elasticity in the substrate

Chen, X., Hutchinson, J.: Herringbone buckling patterns of compressed thin films on compliant substrates. Journal of Applied Mechanics 71, 597–603 (2004)

# Resolution using ANM

- Notations :

- Displacement field :  $\mathbf{u}$
- Green Lagrange strain tensor :  $\gamma(\mathbf{u})$
- Second Piola-Kirchhoff stress tensor:  $\mathbf{S} = \mathbf{D} : \gamma$

- Hellinger-Reissner mixed formulation :

$$HR(\mathbf{u}, \mathbf{S}, \lambda) = \int_{\Omega} \left( \mathbf{S} : \gamma(\mathbf{u}) - \frac{1}{2} \mathbf{S} : \mathbf{D}^{-1} : \mathbf{S} \right) d\Omega - \lambda P_e(\mathbf{u}) \quad (1)$$

↓  
 $\frac{1}{2} (\nabla \mathbf{u} + \nabla^T \mathbf{u}) + \frac{1}{2} (\nabla^T \mathbf{u} \cdot \nabla \mathbf{u})$   
 $\gamma_l(\mathbf{u}) \qquad \qquad \qquad \gamma_{nl}(\mathbf{u}, \mathbf{u})$

$\int_{\Omega} \rho \mathbf{b} \cdot \mathbf{u} d\Omega + \int_{\partial\Omega} \rho \mathbf{t} \cdot \mathbf{u} d\Gamma$   
 ↓  
 loading parameter  
 ↓  
 Elasticity tensor

- At the equilibrium  $HR(\mathbf{u}, \mathbf{S}, \lambda)$  is extremal for a fixed  $\lambda$

$$\delta HR(\mathbf{u}, \mathbf{S}, \lambda) = \int_{\Omega} \left( \mathbf{S} : \delta \gamma(\mathbf{u}) + \delta \mathbf{S} : \gamma(\mathbf{u}) - \mathbf{S} : \mathbf{D}^{-1} : \delta \mathbf{S} \right) d\Omega - \lambda P_e(\delta \mathbf{u}) = 0 \quad (2)$$

↓  
 $\gamma_l(\delta \mathbf{u}) + 2\gamma_{nl}(\mathbf{u}, \delta \mathbf{u})$

# Resolution using ANM

- Définition of  $\mathbf{U} = \begin{pmatrix} \mathbf{u} \\ \mathbf{S} \end{pmatrix}$ , mixed variable (3)
- ANM consists in Talor series expansion with respect to a path parameter  $a$  :

$$\begin{cases} \mathbf{U}(a) = \mathbf{U}^j + a\mathbf{U}_1 + a^2\mathbf{U}_2 + \mathbf{L} \\ \lambda(a) = \lambda^j + a\lambda_1 + a^2\lambda_2 + \mathbf{L} \end{cases} \quad (4)$$

At the begin of the  $j^{\text{th}}$  branch

- Choice of the  $a$  : linearized arc length :

$$a = \langle \mathbf{u} - \mathbf{u}^j, \mathbf{u}_1 \rangle + (\lambda - \lambda^j) \lambda_1 \quad (5)$$

- Using series development (4) in (2), at the order  $p$  in  $a$ , we obtain the variational formulation (FV) :

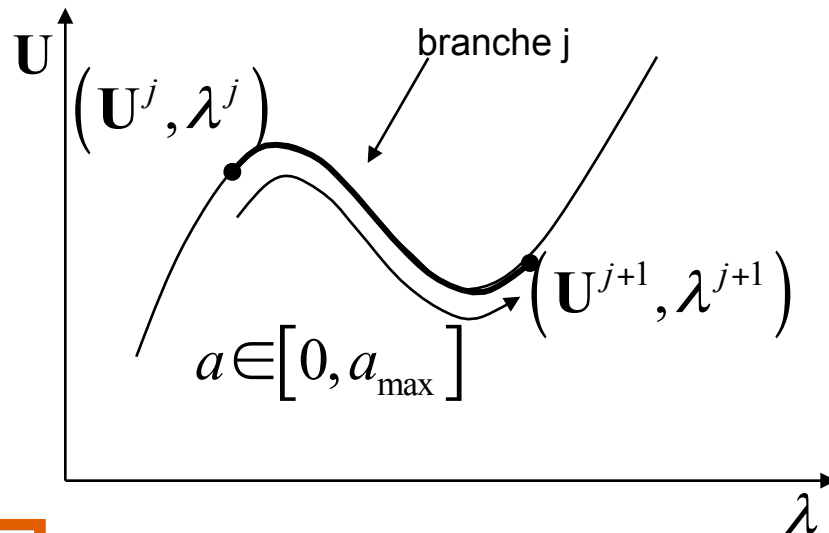
$$\int_{\Omega} \left( \delta \gamma(\mathbf{u}^j) : \mathbf{D} : \left( \gamma_l(\mathbf{u}_p) + \gamma_{nl}(\mathbf{u}^j, \mathbf{u}_p) \right) + \mathbf{S}^j : 2\gamma_{nl}(\mathbf{u}_p, \delta \mathbf{u}) \right) d\Omega = \lambda P_e(\delta \mathbf{u})$$

$$- \int_{\Omega} \left( \left( \sum_{r=1}^{p-1} \mathbf{S}_r : 2\gamma_{nl}(\mathbf{u}_{p-r}, \delta \mathbf{u}) \right) + \left( \sum_{r=1}^{p-1} \gamma_{nl}(\mathbf{u}_r, \mathbf{u}_{p-r}) \right) : \mathbf{D} : \delta \gamma(\mathbf{u}^j) \right) d\Omega \quad (6)$$

# Resolution using ANM

- from (5), it results :
  - at order (1),  $\langle \mathbf{u}_1, \mathbf{u}_1 \rangle + \lambda_1 \lambda_1 = 1$  (7)
  - at l'order (p),  $\langle \mathbf{u}_p, \mathbf{u}_1 \rangle + \lambda_p \lambda_1 = 0$
- if N is the development order of the serie (de 15 à 50), by estimating the convergence radius of the serie, we derive a maximum value  $a_{\max}$  for each branch :

$$a_{\max} = \left( \delta \frac{\|\mathbf{u}_1\|}{\|\mathbf{u}_N\|} \right)^{\frac{1}{N-1}} \quad (8)$$



→ Small steps indicate a bifurcation point

# 2D FEM implementation using FreeFem++

- FEM can be successfully used to implement ANM for the resolution the non linear film/substrate mechanical problem
- FEM implementation has been realized using **FreeFem++**
- P2 Lagrange triangular finite element has been used :
  - Few finite element in the film thickness
  - almost 10 elements in the substrate thickness
  - A few hundred in the film length
- Definition of linear and non linear parts of Green Lagrange tensors and its differential using **macro** :

```
macro GammaL(u,v) [dx(u),dy(v),(dy(u)+dx(v))] //
```

```
macro GammaNL(u1,v1,u2,v2) [ ··· ] //
```

```
macro Gamma(u,v) (GammaL(u,v)+GammaNL(u,v,u,v)) //
```

```
macro dGammaNL(u,v,uu,vv) (2.0*GammaNL(u,v,uu,vv)) //
```

```
macro dGamma(u,v,uu,vv) (GammaL(uu,vv)+dGammaNL(u,v,uu,vv)) //
```

# 2D FEM implementation using FreeFem++

- Define elasticity matrices in FreeFem++  $\mathbf{D}_s$   $\mathbf{D}_f$
- At the **first order** in p, FEM allows to transform FV (6) in a linear system :

$$\begin{array}{c} \text{Nodal displacement vector} \\ \downarrow \\ \mathbf{K}_t \hat{\mathbf{U}}_1 = \lambda_1 \mathbf{F} \\ \nearrow \text{tangent matrix} \quad \searrow \text{second member vector} \end{array} \quad (9)$$

- let us define :  $\hat{\mathbf{U}}_1 = \mathbf{K}_t^{-1} \mathbf{F}$

- using (7), it results :  $\lambda_1 = 1 / \sqrt{1 + \langle \hat{\mathbf{U}}_1, \hat{\mathbf{U}}_1 \rangle}$  et  $\mathbf{U}_1 = \lambda_1 \hat{\mathbf{U}}_1$

- at the order p, it is necessary to build the non linear second member vector  $\mathbf{F}_{nl}$

$$\mathbf{K}_t \mathbf{U}_p = \lambda_p \mathbf{F} + \mathbf{F}_{nl}$$

- Let us define  $\mathbf{U}_{nl} = \mathbf{K}_t^{-1} \mathbf{F}_{nl}$  and from (7), we get  $\lambda_p = -\lambda_1 \langle \mathbf{U}_1, \mathbf{U}_{nl} \rangle$

$$\mathbf{U}_p = \frac{\lambda_p}{\lambda_1} \mathbf{U}_1 + \mathbf{U}_{nl}$$

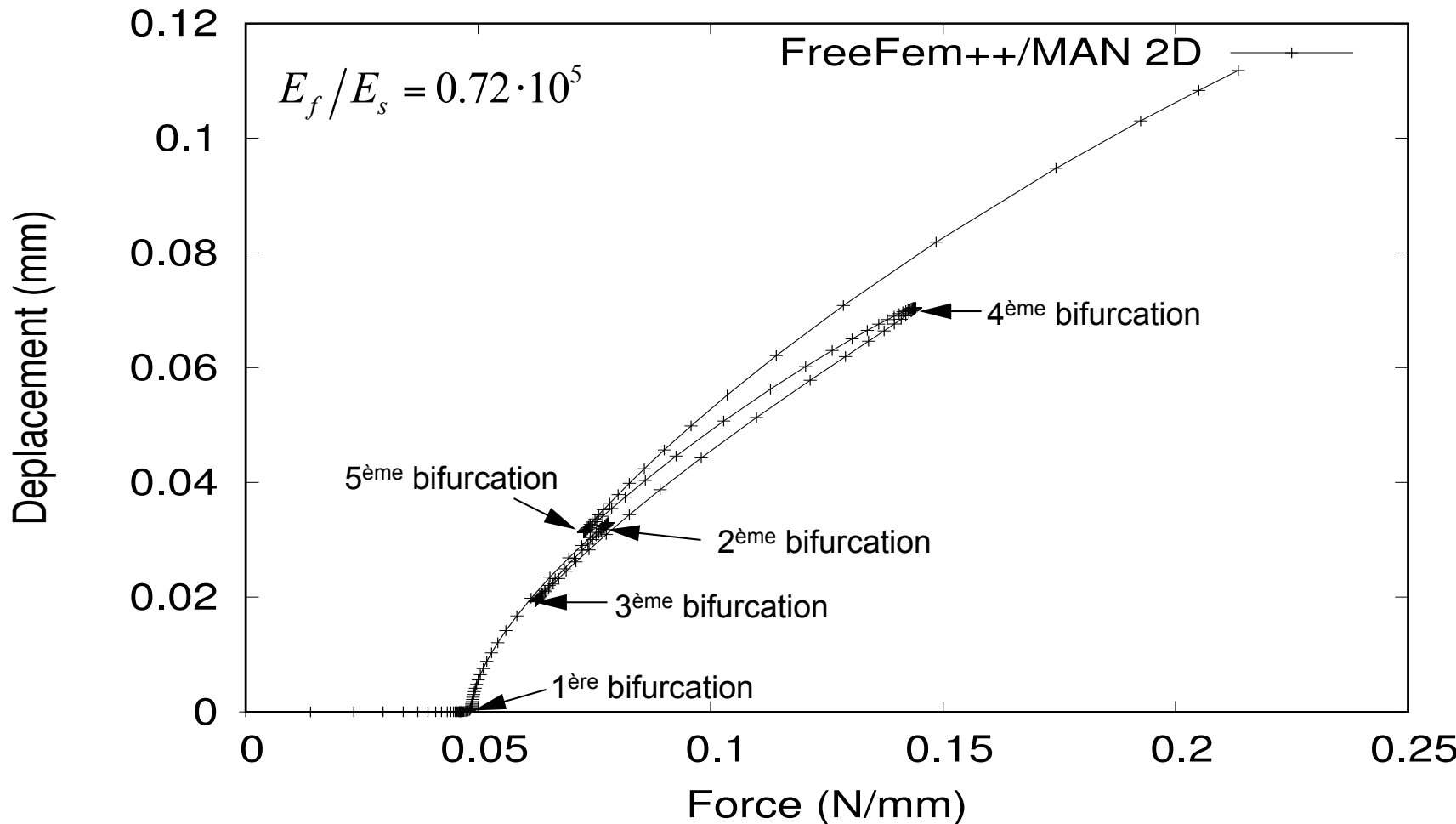
# 2D FEM implementation using FreeFem++

- using previous defined **macro** and the FreeFem++ **varf** command it is possible to obtain :
  - ▶ the tangent matrix  $\mathbf{K}_t$
  - ▶ the second member  $\mathbf{F}_t$
  - ▶ for each order the non linear seond member  $\mathbf{F}_{nl}$
- solve the linear system using UMFPACK, MUMPS
- FreeFem++ parallele mpi code development:
  - ▶ mesh partitioning using **scotch** or **metis**
  - ▶ affect each processor to a part of the mesh, it is necessary to change the **varf**
  - ▶ parallel resolution of the linear system using **MUMPS**

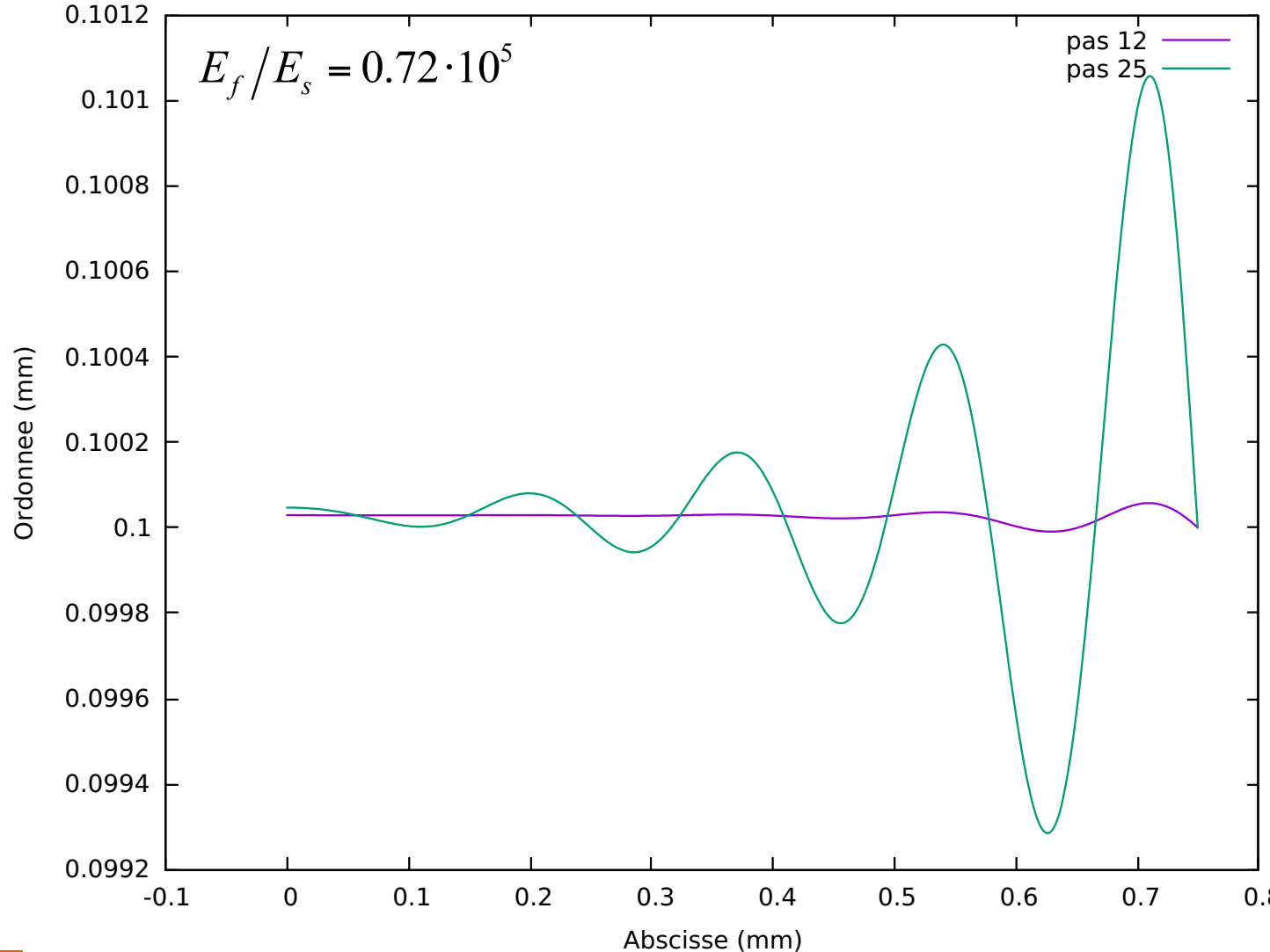
# Numerical results – 2D model

- results obtained during H. Rezgui-Chaabouni's master thesis in 2016
- Finite element mesh : 600 (resp. 100) elements in the length (resp. width) of the substrate, et 600 (resp. 1) elements in the length (resp. width) of the film
- two cases :  $E_f/E_s = 0.72 \cdot 10^5$  and  $E_f/E_s = 0.72 \cdot 10^4$
- Plot of the vertical displacement (top surface of the film)
- Plot of the deformed top surface for various ANM steps

# Numerical results – 2D model

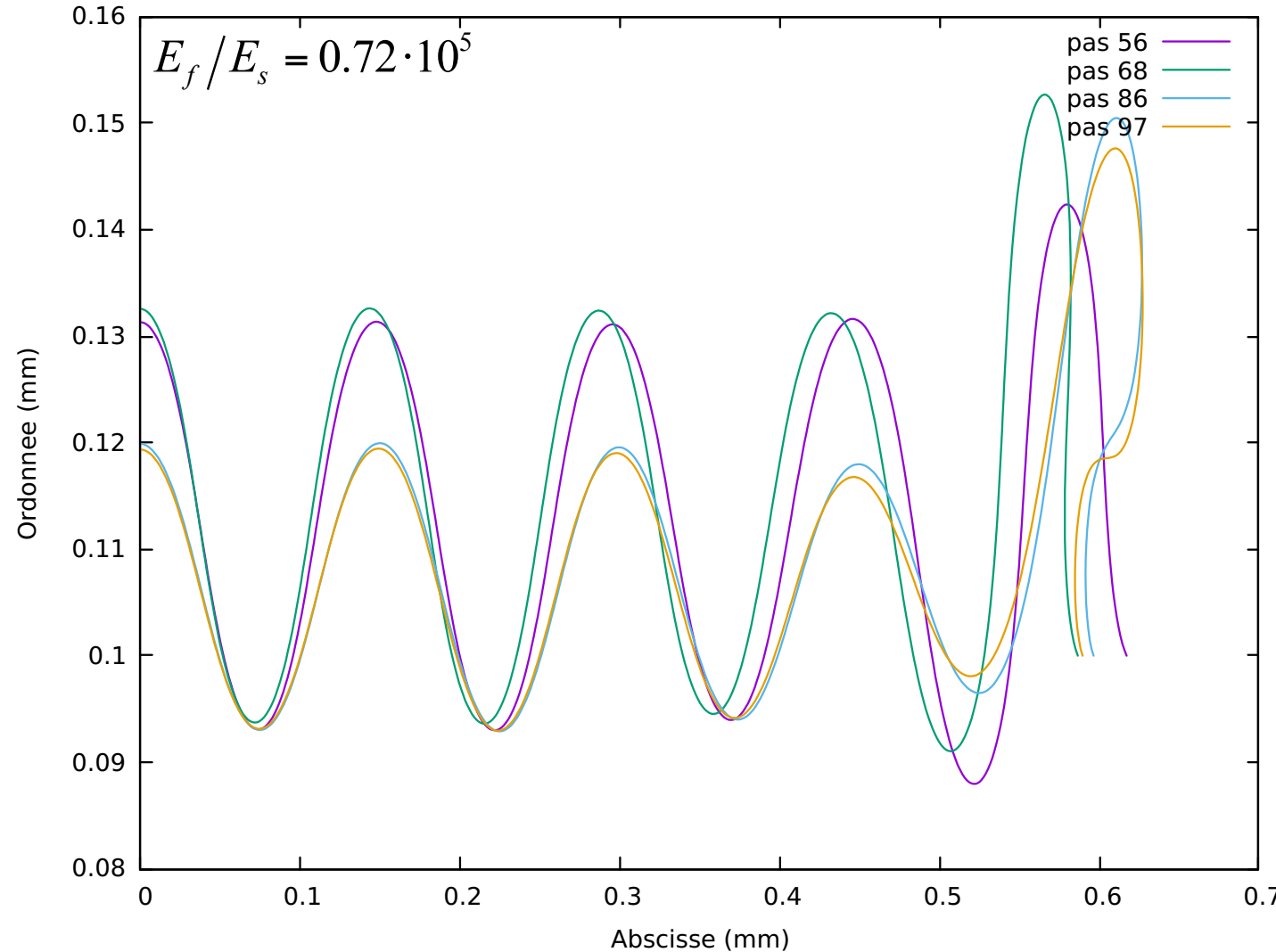


# Numerical results – 2D model

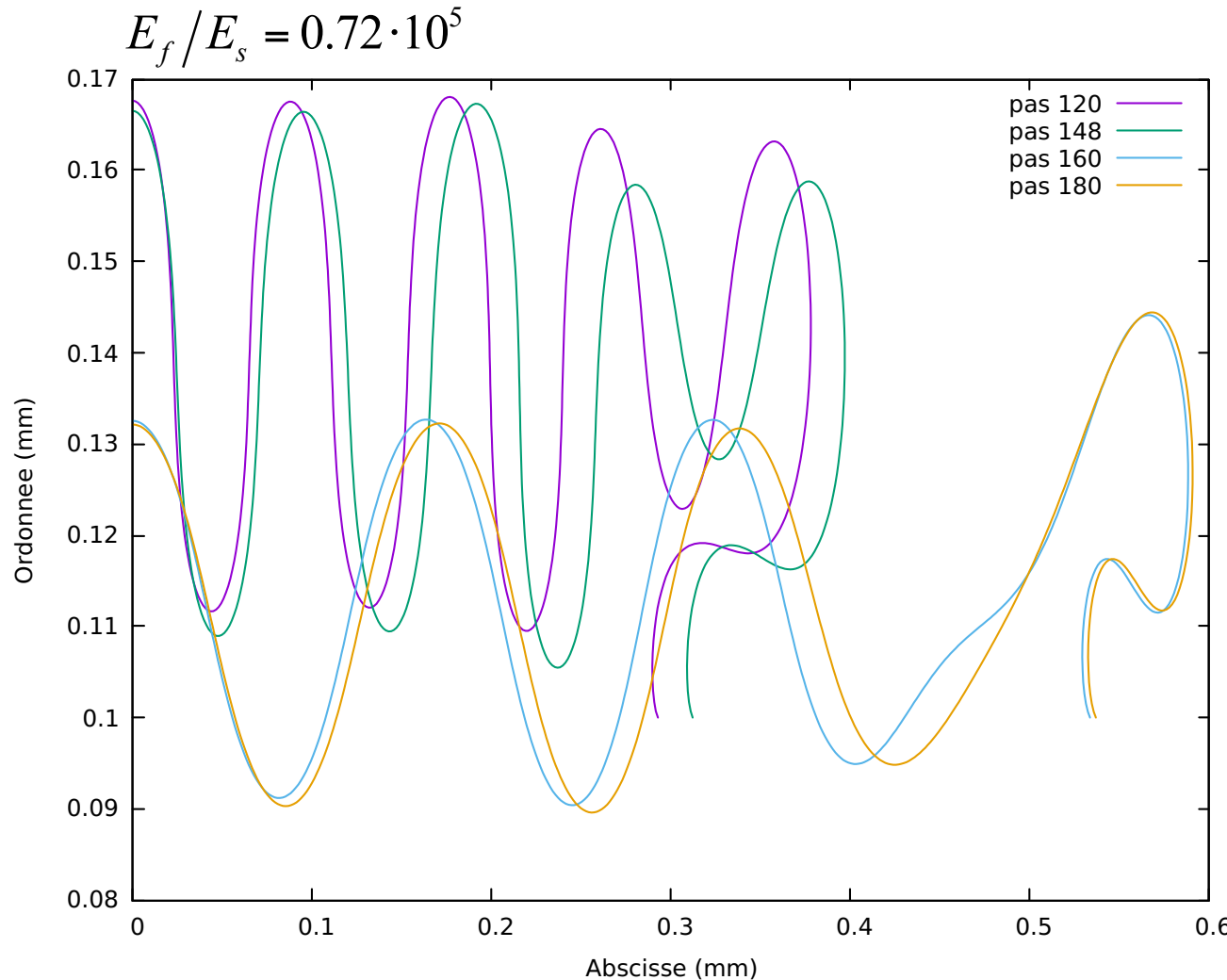


Deformed top surface of the film, before 1<sup>st</sup> bifurcation (step 12, 25)

# Numerical results – 2D model

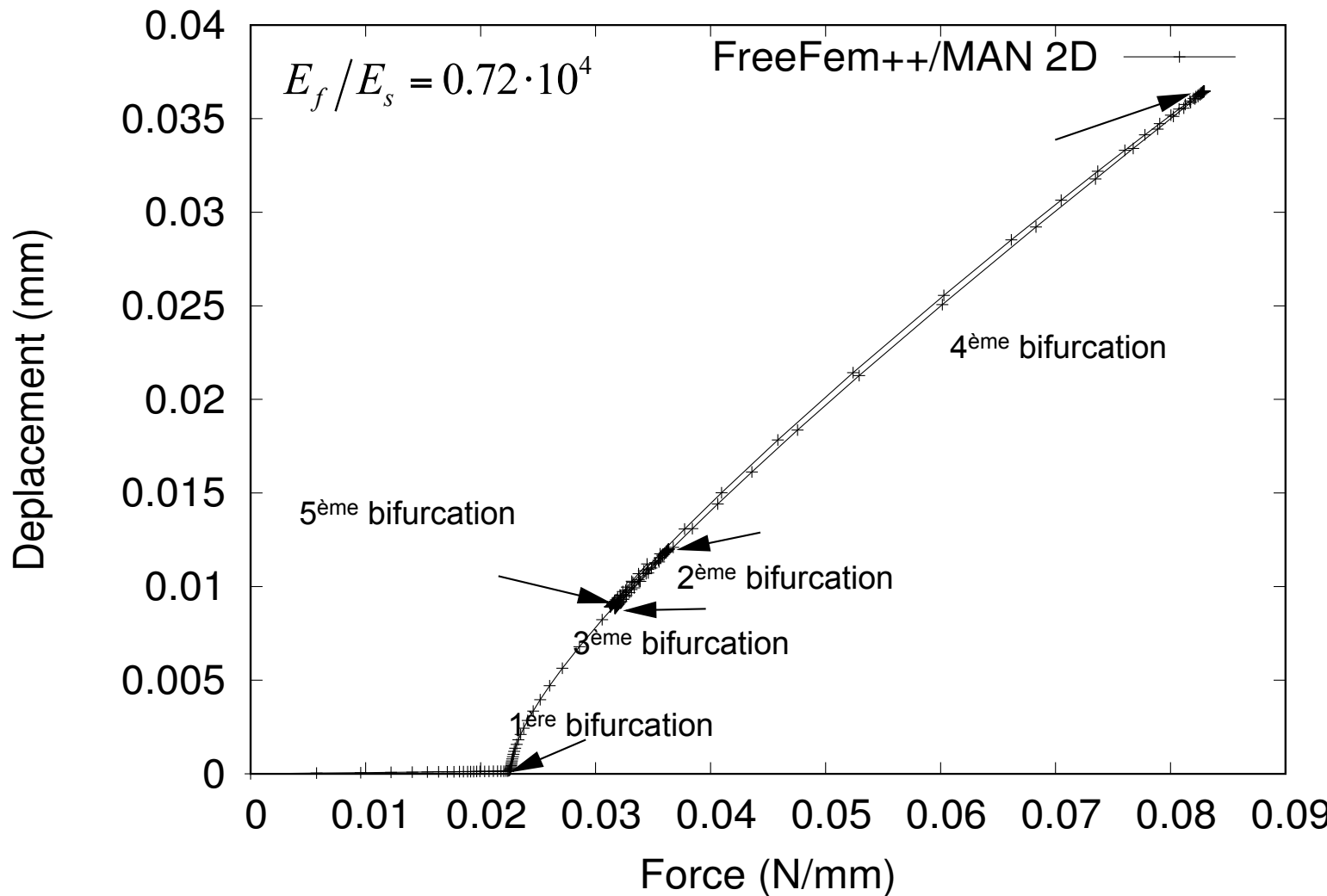


# Numerical results – 2D model



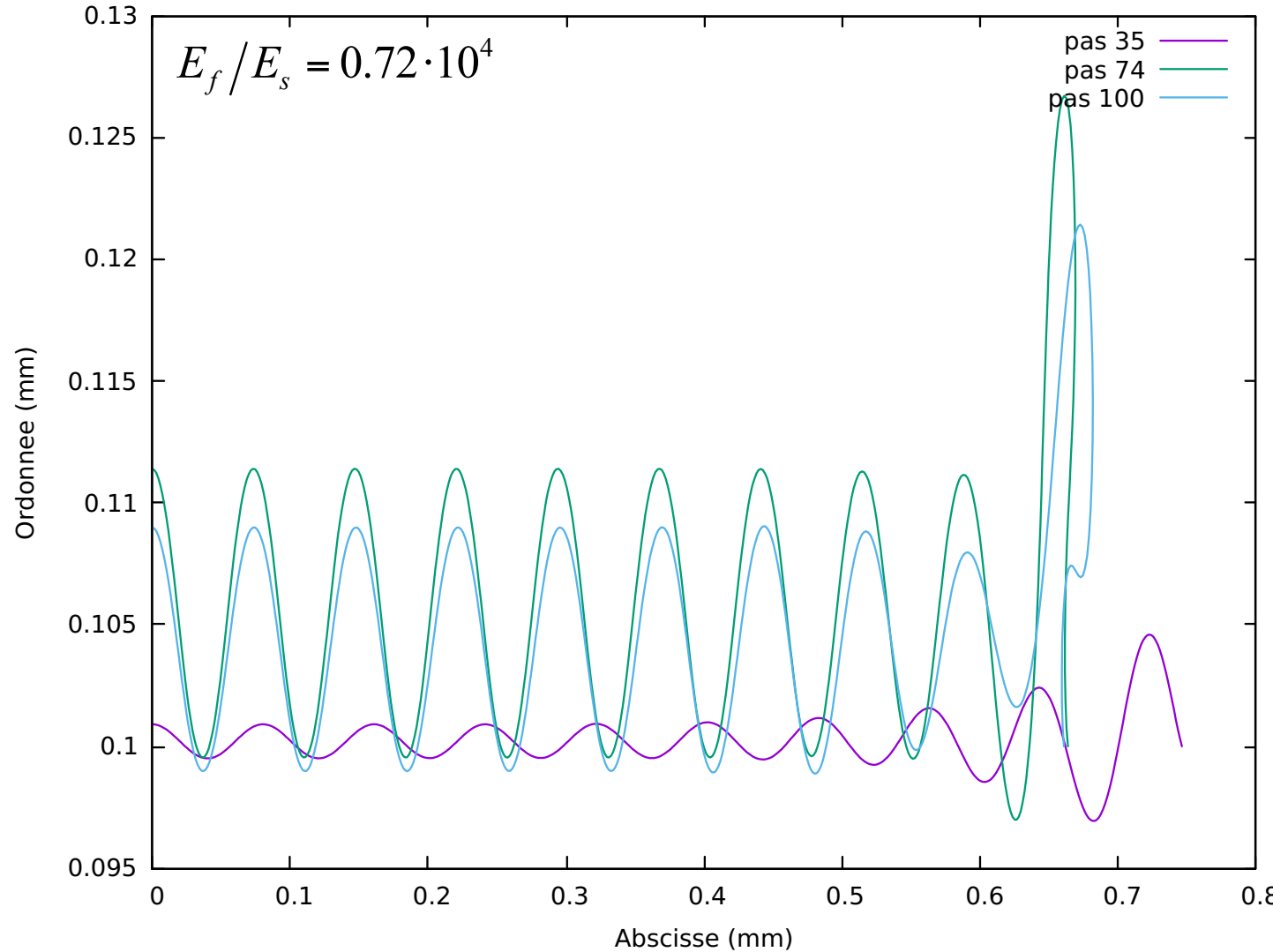
Deformed top surface of the film, before and after the 4<sup>th</sup> (step 120 and 148) and the 5<sup>th</sup> (step 160 and 180) bifurcation

# Numerical results – 2D model



Vertical displacement in the middle of the film (top surface), 200 ANM steps

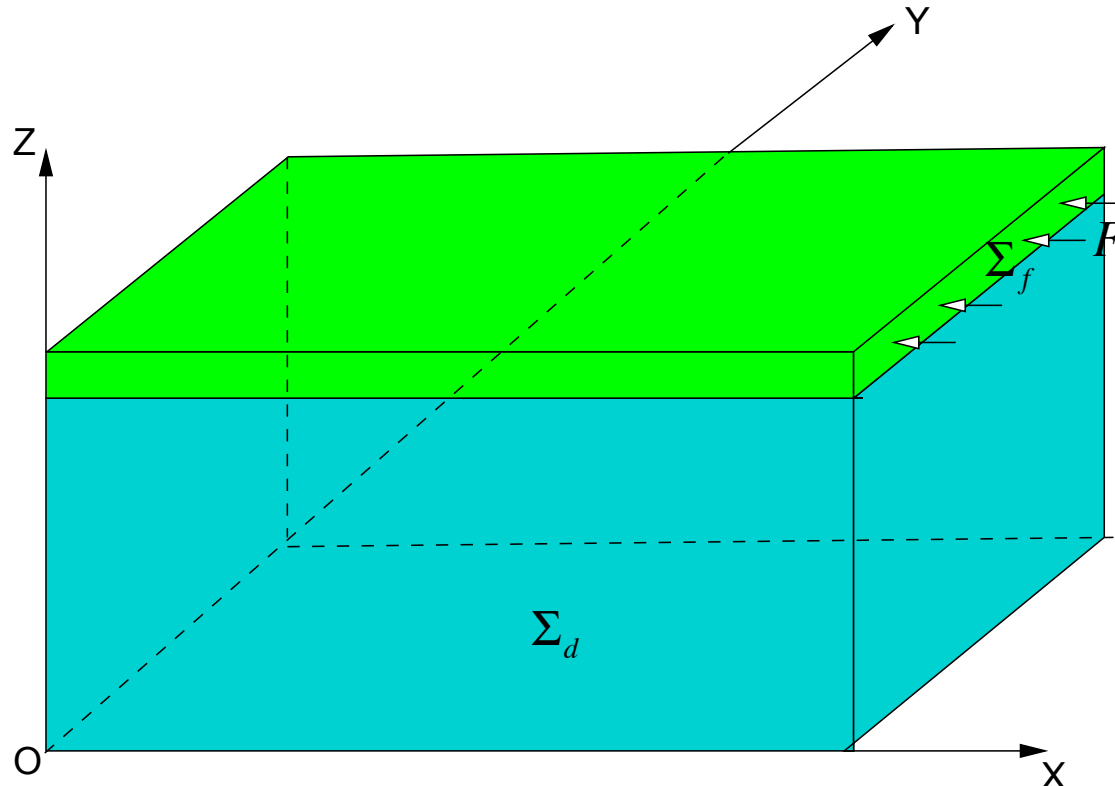
# Numerical results – 2D model



Deformed top surface of the film, after the 1<sup>st</sup> bifurcation (step 35), 2<sup>nd</sup> (step 74), and the 3<sup>rd</sup> (step 100) bifurcation

# Generalized 3D model

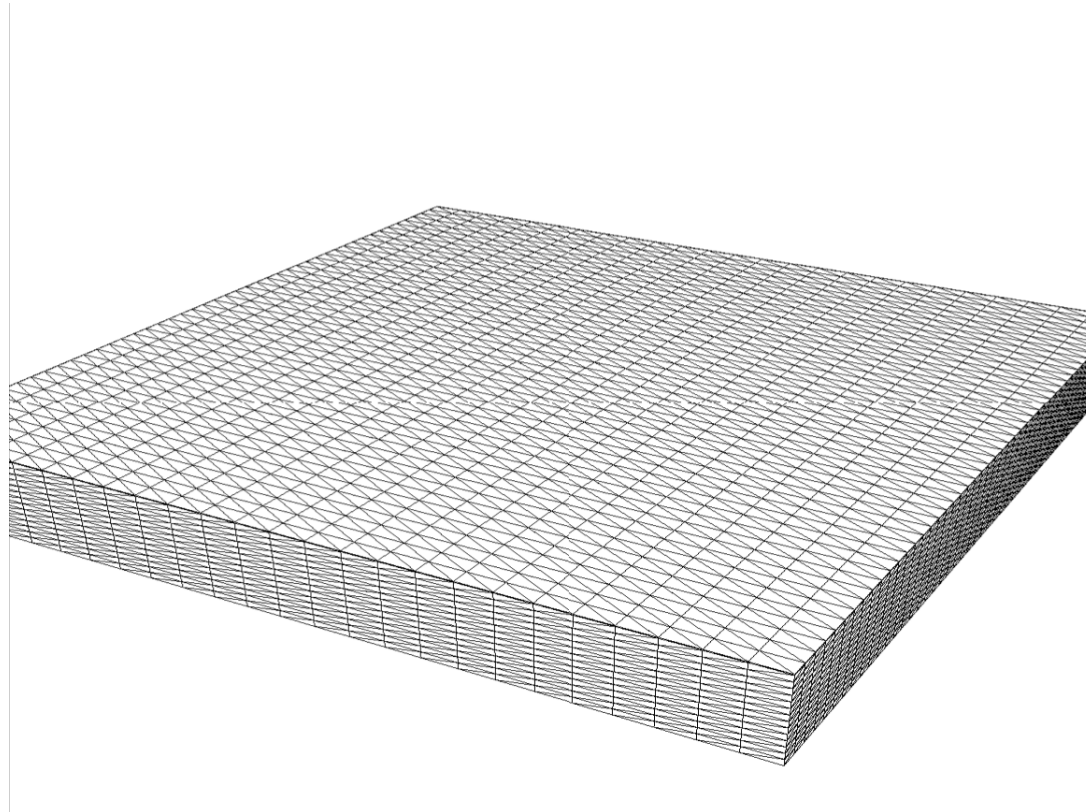
- It is important to develop a 3D model to get more accuracy in the computation of loading curves, the deformed surfaces, and the bifurcations.



- (O,Y,Z) et (O,X,Z) are symmetry planes
- For the below surface  $\Sigma_d$  and the surface  $\Sigma_f$  where the force is applied the vertical displacement is zero.

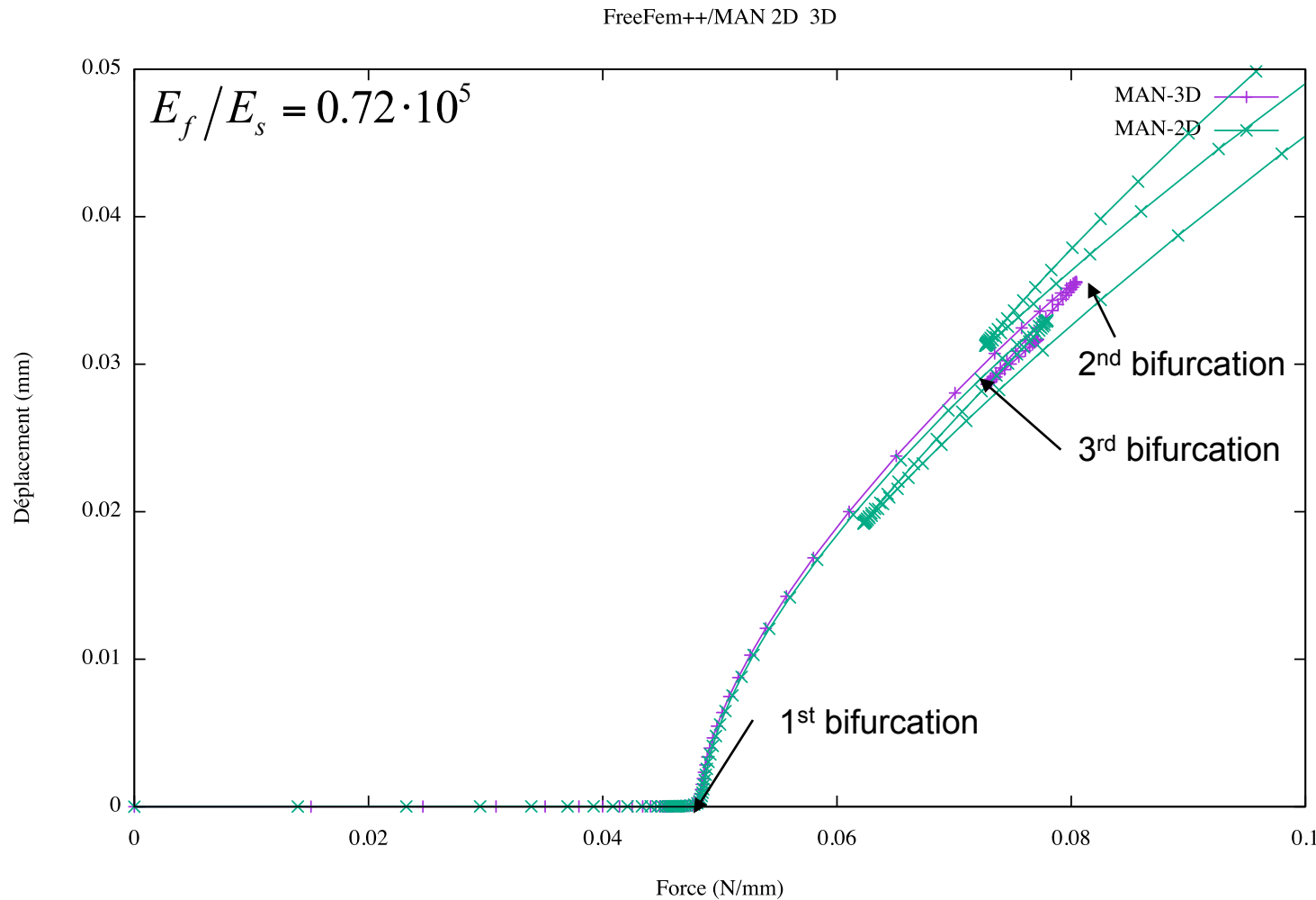
# Généralisation à un modèle 3D

- Use P2 Lagrange tetrahedron finite elements



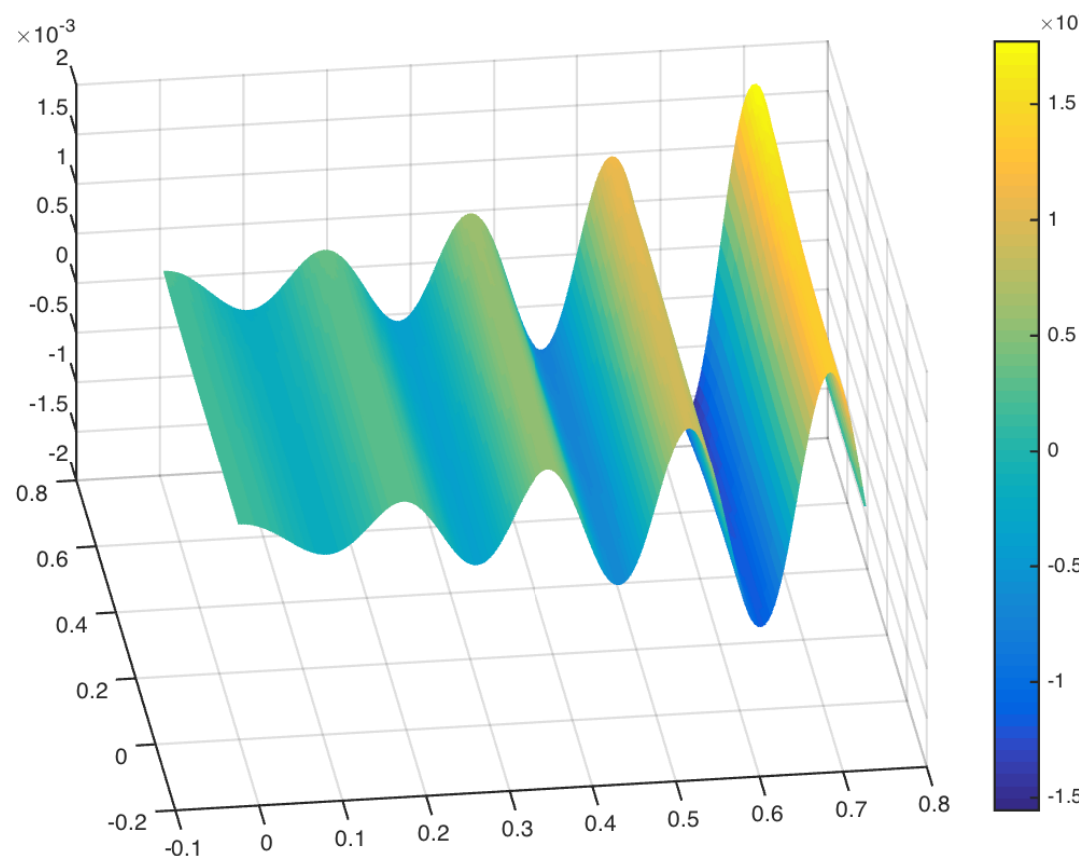
3D mesh of the film substrate system

# Résultats numériques - Modèle 3D



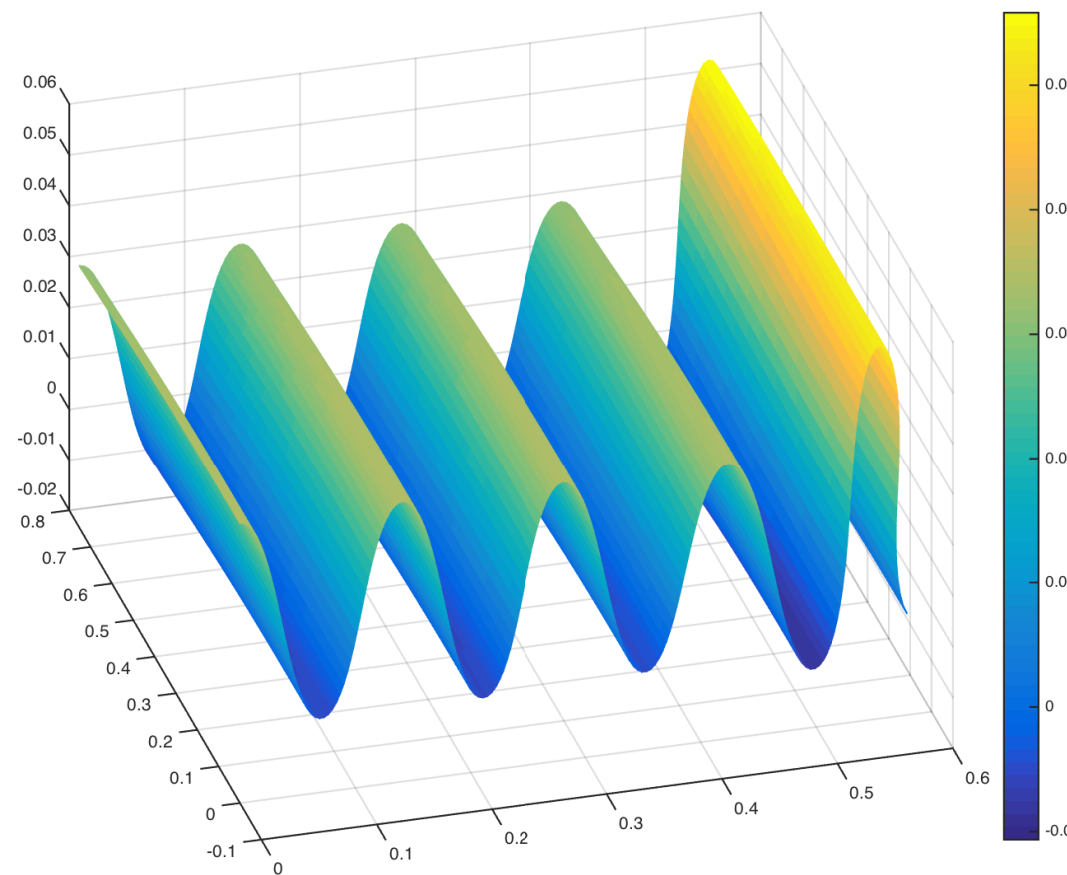
Vertical displacement if the middle of the film (top surface), 200 ANM steps

# Numerical model- 3D model



Deformed top surface of the film after the 1<sup>st</sup> bifurcation (step 32)

# Numerical results- 3D Model



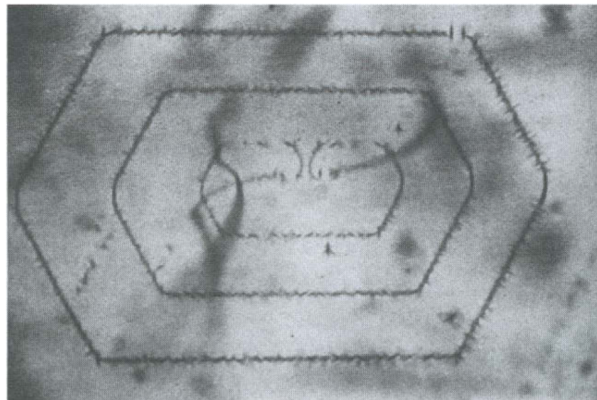
Deformed top surface of the film after the 2<sup>nd</sup> bifurcation (step 70)

# Conclusions

- It has been shown that the study of non linear mechanical problem for solids can be realized successfully using FEM and ANM
- An efficient FreeFem++ parallel code has been implemented in 2D and 3D
- It allowed to study wrinkles in film/substrate systems
- Bifurcation curves, and deformations at the top of the film has been shown
- Future work : improve parallel scalability using Domain Decomposition Method

- Utilisateurs LEM3 : V. Taupin, P. Ventura, T. Richeton, L.T. Le, K.S. Djaka
- Utilisateur Georgia Tech Atlanta & Los Alamos National Laboratory
- Utilisation dans le cadre d'une collaboration avec : LGGE, CEMEF, Russian Academy of Sciences, Georgia Tech Atlanta, Los Alamos National Laboratory, Constellium C-Tech

Multiplication of dislocation loops  
Frank Read Source (observation exp.)



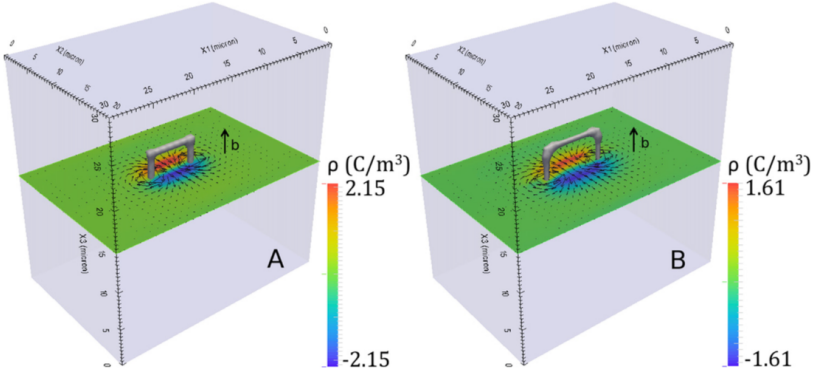
Dislocation transport equation  
Least-Squares weak form

$$\dot{\alpha} = -\text{curl} (\alpha \times \mathbf{v})$$

$$\begin{aligned} \delta \alpha_{ri}^A \left[ \int_V N^A N^B \alpha_{ri}^{Bt+\Delta t} \, dV - \int_V N^A \alpha_{ri}^t \, dV + \Delta t \int_V N^A L_{ri}^t \, dV \right. \\ + \Delta t^2 \int_V [M_{pqri}^e(N^A v_j^e),_j - M_{pjri}^e(N^A v_q^e),_j] L_{pq}^t \, dV \\ + \Delta t^2 \int_V [M_{pqri}^s(N^A v_j^s),_j - M_{pjri}^s(N^A v_q^s),_j] L_{pq}^t \, dV \\ \left. + \Delta t \int_{S_i} |v_k n_k| N^A (\alpha_{ri}^t - \bar{\alpha}_{ri}) \, dS \right] = 0. \end{aligned}$$

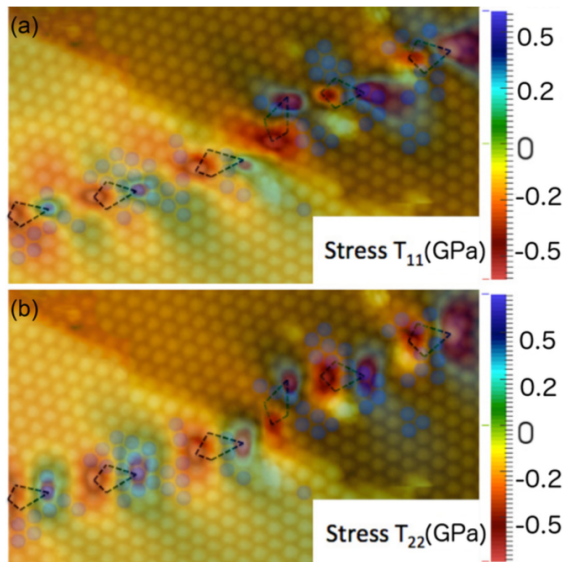
- Frank\_Read\_source.edp : simulation 2D
- Equations dans K.S. Djaka et al, MSMSE 23, 065008 (2015)
- Weak form : S. Varadhan et al, MSMSE 14, 1245-1270 (2006)

## Dislocations et piézoélectricité



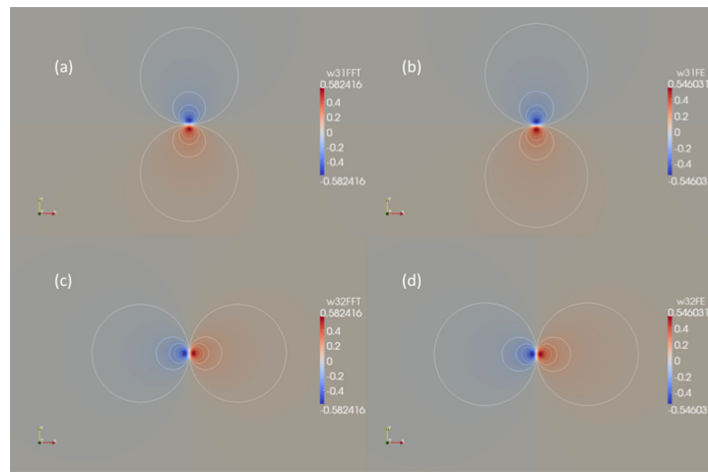
V. Taupin et al, JAP 115, 144902 (2014)

## Désinclinaisons dans les fullerènes



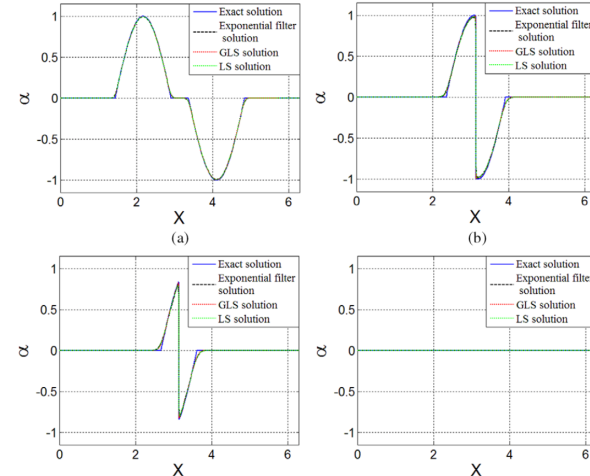
S. Bozhko et al, PRB 90, 214106 (2014)

## Champs élastiques de dislocations Comparaison FFT (gauche) / FEM (droite)



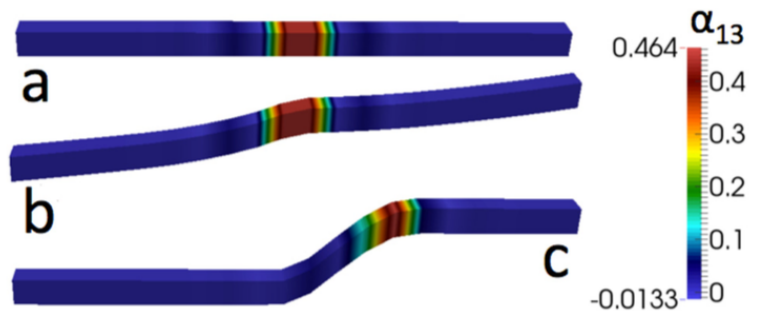
S. Berbenni et al, IJSS 51, 4157-4175 (2014)

## Equation de transport, comparaison FFT / FEM



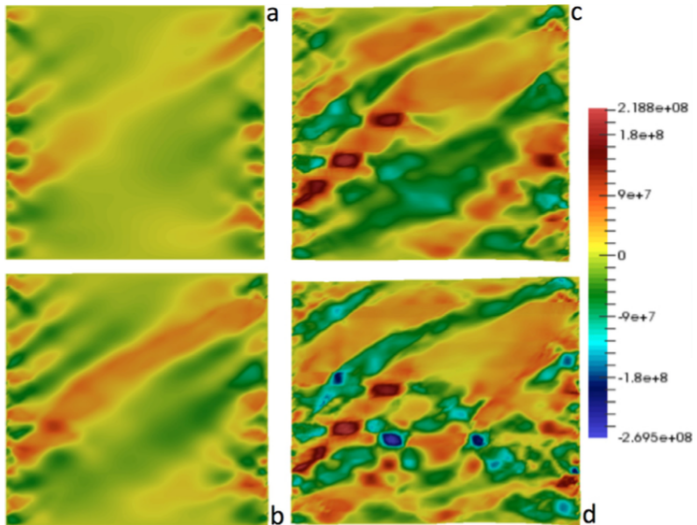
K.S. Djaka et al, MSMSE 23, 065008 (2015)

## Résolution d'équations de transport Migration des joints de grains



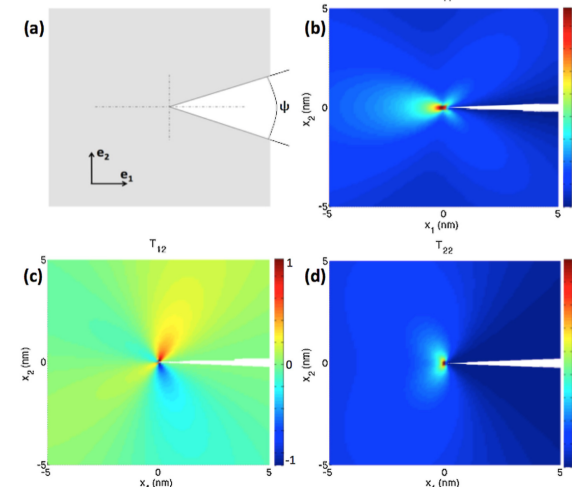
V. Taupin et al, IJSS 71, 277-290 (2015)

## Plasticité cristalline Localisation dans les alliages Al-Cu-Li



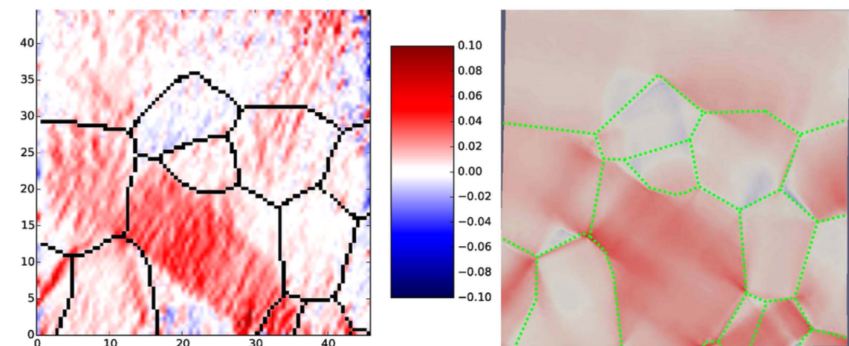
V. Taupin et al, IJSS 99, 71-81 (2016)

## Mécanique de la fracture



C. Fressengeas et al, IJSS 82, 16-38 (2016)

## Plasticité polycristalline dans la glace



T. Richeton et al, MSMSE 25, 025010 (2017)

# Thank you for your attention